Diode-switched thermal-transfer printed antenna on flexible substrate

Diode-switched thermal-transfer printed antenna on flexible substrate

M. Kgwadi and T. D. Drysdale

We demonstrate that diode-switching can be used to introduce frequency agility into antennas produced by thermal transfer printing. Our particular example is a triangular Sierpinski fractal pattern with two PIN diodes to switch between operation optimised for the 800 MHz UHF band (diodes on) and the 2400 MHz ISM band (diodes off). Our measured results show an improvement in S_{11} in the UHF band from -2 dB to -28 dB, and from -7 dB to -30 dB at 2400 MHz, when switching the diodes appropriately. The measured bandwidth is 200 (1000) MHz, and the measured directivity is 3.1 dB (5.2 dB) while the measured gain is -5.2 dB (6.7 dB) for the diodes on(off).

Introduction: Rapid and inexpensive antenna manufacturing is required to support the burgeoning interest in the Internet of Things (IoT). IoT is heavily reliant upon wireless communications between, ultimately, trillions of devices [1]. For any IoT antenna, it is important to be able to handle a dynamic frequency allocation, at least in part determined by regulatory authorities according to location [2] but also influenced by the local propagation environment favouring some channels over others due to fading mechanisms associated with building geometry e.g. [3] and other radio noise sources. Hence, reconfigurable antennas are attractive both for prototyping IoT communications networks in new locations, but also during deployment for responding to changes in the optimal channel choice. Reconfigurable antennas often require less non-returnable engineering effort compared to designing multi-band antennas, and can go further than frequency agility to include polarisation diversity [4] or beamforming capability [5]. Switching is known to introduce frequency [6] and polarisation [7] agility into planar antennas produced using conventional printed circuit board techniques on a variety of dielectric substrates. However, these manufacturing techniques are relatively slow compared to thermal transfer printing of metallic films, which prints at a rate of approximately 5cm/s and requires no curing to reach minimum sheet resistance [8]. Flexible substrates give IoT system designers more options for integrating nodes unobtrusively into built environments [9].

Antenna design and implementation: An IoT antenna needs to be able to switch between two or more different bands depending on spectrum allocation from regulatory authorities, spectrum availability due to other users, or deleterious effects in the local propagation environment. A sequentially reconfigurable frequency agile Sierpinski antenna using RF microelectro-mechanical systems (RF MEMS) switches was achieved in [10]. The RF MEMS in [10] require DC bias voltage of up to 17 V to achieve switching, which may not be cost effective in low power sensor nodes. Therefore PIN diodes are an attractive alternative for our approach because they can be switched with voltages lower than 1 V DC (nominal value 0.95 V) [11]. We propose a Sierpinski gasket-based tunable antenna using NXP semiconductor's general purpose PIN diodes (BAP50-03) as switches, so as to allow a sensor node to switch between ISM band (2400 MHz) communications and the television white space (TVWS) bands centered at (800 MHz) by using a flexible, low-cost frequency agile antenna. Thus an associated sensor node could switch between the two frequency bands depending on availability and/or network traffic conditions. Figure 1(a) shows a schematic of our design, with a photograph of the final printed version shown in Figure 1(b). The antenna was printed using thermal-transfer printing by a Zebra S4 300 dpi, on a Flexcon THERMfilm® SELECT 21944E which is a polyester with relative dielectric constant (ε_r) of 3.2 [8]. The metalization was achieved by IIMAK's Metallograph™ conductive thermal transfer ribbon which yields a 260 nm aluminium layer. The antenna is switched between the 'ON' and 'OFF' state by switch *S*, via a voltage supply fed through the vector network analyser DC-bias port. On a microcontroller-based sensor node, the same can be achieved by programming one of the output pins. For a 3.3 V output pin voltage, a 47 Ω resistor in series with the PIN diode will be required obtain the required forward bias current of 50 mA. In the 'ON' state the diodes are forward biased and the whole of the antenna is in operation, resonating at 800 MHz. In the 'OFF' state the diodes are at zero bias and the antenna elements beyond the cathodes of the diodes are effectively disconnected, yielding a shorter antenna that resonates at

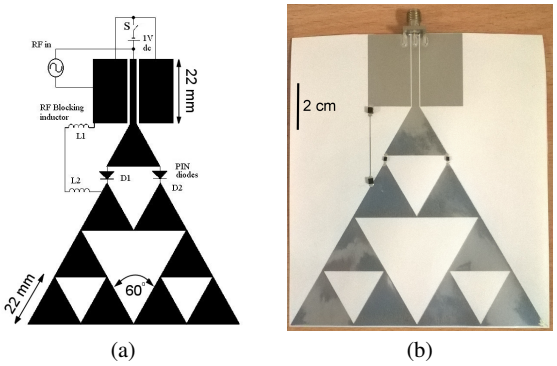

Fig. 1 *Schematic (a) of the reconfigurable Seirpenski antenna (dimensions: CPW center strip 3.2 mm, CPW gap 0.35 mm, CPW ground width 18 mm) and picture (b) of the fabricated antenna.*

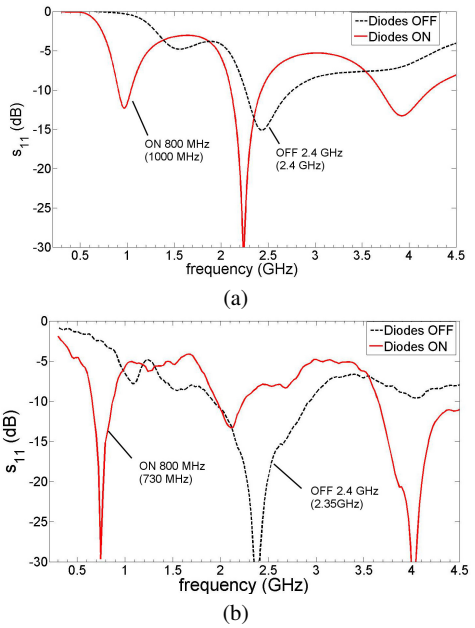

Fig. 2 *Plots of S_{11} parameter for the (a) simulated and (b) measured antennas, for the diodes ON and OFF. With the diodes OFF, operation is at 2.4 GHz and ON at 800 MHz (larger effective structure size).*

2400 MHz. In practice, some residual loading remains because the diode is not a perfect open circuit. Two surface-mount inductors are used to isolate the RF signal from the ground.

Simulation and measurements: The antenna was simulated in openEMS which is an open source, finite-difference time-domain based electromagnetic field solver [12]. The metallisation was modelled as a perfect electrical conductor of infinitesimal thickness to give reasonable simulation times. This does not affect the radiation pattern or operating frequency but prevents us from predicting the efficiency. Lumped components were used to model the PIN diodes and inductors in the simulations. The reverse bias capacitance of the diodes was modelled as a 0.4 pF lumped capacitor in the 'OFF' state, while the forward bias resistance was modelled as a 3 Ω lumped resistor in the 'ON' state. The inductor was modelled as lumped 4.7μH inductance in series with a 3 Ω resistance. Figure 2(a) shows the simulated reflection coefficient in the two cases when the diodes are 'ON' and 'OFF'. Figure 2(b) shows the measured S_{11}, with the desired resonance in the ISM band (WLAN, 2400-2500 MHz) with an S_{11} better than -30 dB through the entire band and no resonance at 800 MHz in the 'OFF' state. In the 'ON' state, the resonance in UHF band is observed at 730 MHz with an S_{11} of -28 dB and operational bandwidth of 200 MHz ($S_{11} \leq$-10 dB). The 150 MHz shift in the resonance frequency between simulation and measurements is attributed to discretization of the diagonal lines into a staircase approximation and the presence of a 56 μm glassine liner which preserves the acrylic adhesive and thus makes the structure electrically larger than simulated (hence the resonances shifts to the lower frequencies).

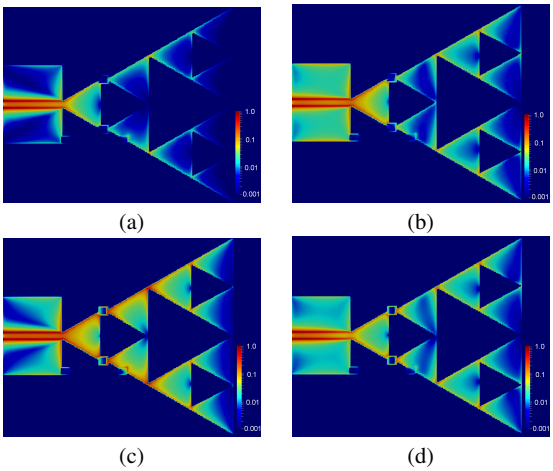

Fig. 3 *Simulated normalized current densities, (a) at 800 MHz in the 'OFF' state,(b) 2400 MHz in the 'OFF' state,(c) 800 MHz in the 'ON' state , and (d) 2400 MHz in the 'ON' state.*

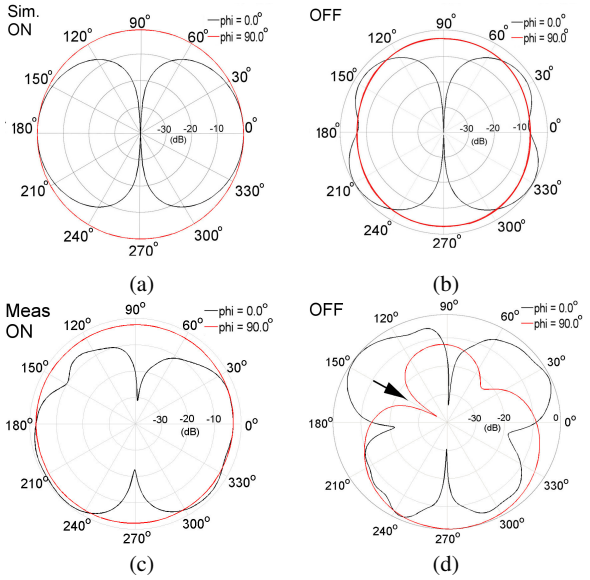

Fig. 4 *Simulated and measured radiation patterns. (a) simulated radiation pattern at 800 MHz in the 'ON' state and (b) simulated radiation patterns at 2400 MHz in the 'OFF' state; (c) corresponding measured radiation pattern in the 'ON' state at 800 MHz and (d) measured radiation pattern in the 'OFF' state at 2400 MHz. The arrow marks a null caused by the bias line.*

The glassine liner, whose dielectric permittivity is unknown to us, was omitted in the simulations since it is expected to be peeled off during antenna deployment. Our measured results are sufficient to demonstrate the principle, although we would expect some fine tuning to the design would be needed to take into account the precise conditions under which it was manufactured in volume.

Figure 3 shows the normalised surface current distribution in both 'ON' and 'OFF' cases at the two design frequencies. In the 'OFF' state the current density at 800 MHz is limited to the lower part of the antenna as shown in Figure 3(a). The current distribution at 2400 MHz shown Figure 3(b) shows a higher intensity in the active part of the antenna compared to 800 MHz in Figure 3(a) signifying resonance. Some currents also appear on the inactive part of the antenna in the 'OFF' state, due to fringing capacitance. In the 'ON' state, the 800 MHz current is distributed through out the whole antenna as shown in Figure 3(c) and shows higher intensity than in the 'OFF' state. This shows the antenna resonating at 800 MHz in the 'ON' state. Figure 3(d) shows the current distribution at 2400 MHz.

The radiation pattern was measured using an NSI 2000 near field spherical scanner in a 4.5x4.5x4.0 m anaechoic chamber. The normalized simulated far-field radiation patterns for 800 MHz ('ON') and 2400 MHz ('OFF') are shown in Figure 4(a) and Figure 4(b) respectively. The corresponding normalized measured far-field radiation patterns at 800 MHz ('ON') and 2400 MHz ('OFF') are shown in Figure 4(c) and Figure 4(d) respectively. The measured radiation patterns in the 'ON' state are omnidirectional with a measured gain of -5.3 dBi and a directivity of 3.1 dB at 800 MHz. The low measured gain is attributed to the conductor losses due to thin metallization (0.07 of the skin depth) typical of printed antennas [13] and losses in the resistances of the forward biased PIN diodes and RF blocking inductors. The radiation pattern is however consistent with the simulated radiation pattern in Figure 4(a). The measured radiation pattern at 2400 MHz ('OFF') shows omnidirectional radiation pattern as shown in Figure 4(d), with a measured gain of 6.7 dB and directivity of 5.2 dB. There is an unexpected null in the measured pattern in the E-Plane at 150^o which we attribute to the presence of bias line of length 2 cm at 2400 MHz (0.16λ) although this is of negligible consequence at 800 MHz (0.05λ).

Conclusion: We present a flexible, low-cost, frequency-agile triangular Sierpesnki gasket-based antenna fabricated by thermal transfer printing for use by wireless sensor nodes in IoT applications. The antenna employs two general purpose PIN diodes, two inductors and a single bias line to switch between two modes of operation. By switching the diodes on or off, the desired frequency agility between the UHF band (800 MHz) and the WLAN band (2400-2500 MHz) is achieved with bandwidths of 200 MHz and 1000 MHz respectively. The radiation pattern is omnidirectional with measured directivity of 3.1 dB (800 MHz/'ON') and 5.2 dB (2400 MHz/'OFF') and measured gains of -5.2 dB (800 MHz/'ON') and 6.7 dB (2400 MHz/'OFF') suitable for use in wireless sensor nodes. We thus show that the benefit of thermal transfer printing can be combined with switching elements to make low-cost, flexible, reconfigurable antennas.

Acknowledgement: We would like to thank IIMAK for donating the Metallograph conductive ribbon.

M. Kgwadi (Division of Electronics and Nanoscale Engineering, University of Glasgow, Glasgow, G12 8LT,UK.)
T. D. Drysdale (Department of Engineering and Innovation, The Open University, Milton Keynes, MK7 6AA, UK.)
E-mail: timothy.d.drysdale@ieee.org

References

1 Tan, L. and Wang, N.: 'Future Internet: The Internet of Things', *Adv. Comp. Theory and Eng. (ICACTE), Aug. 2010 3rd Int. Conf.*, 2010, **5**, pp. 476-380.
2 Ofcom: 'TV White Spaces: Approach to coexistance', http://stakeholders.ofcom.org.uk/binaries/consultations/white-space-coexistence/summary/white-spaces.pdf, accessed 28 May 2014.
3 Austin, A., Neve, M., Rowe, G., and Pirkl, R.: 'Modelling the effects of nearby buildings on inter-floor radio-wave propagation', *Anten. and Prop., IEEE Trans.*, 2009, **57**,(7), pp. 2155-2161.
4 Yang, X., Shao, B., Yang, F., Elsherbeni, A. and Gong, B.: 'A Polarization Reconfigurable Patch Antenna With Loop Slots on the Ground Plane', *Anten. and Wireless Prop. Letters, IEEE*, 2012, **11**, pp. 69-72.
5 Kang, W., Lee, S., and Kim, K.: 'Design of Symmetry Beam Pattern Reconfigurable Antenna', *Electronic Letters*, 2010, **46**, pp. 1536-1537.
6 Christodoulou, C., Fieldner, L., Zachou, V., and Anagnostou, D.: 'Planar Reconfigurable Antennas', *Anten. and Prop., EuCAP 2006, First Europ. Conf. on,*, Nov. 2006, pp. 1-7.
7 Cao, Y., Cheung, S., and Yuk, T.: 'A Simple Planar Polarization Reconfigurable Monopole Antenna for GNSS/PCS', *Anten. and Prop., IEEE Trans.*, 2015,**63**, (2), pp. 500-507.
8 Whyte, G., Harrison, D., Cumming, D., and Drysdale, T.: 'Direct Printing of Flexible Metallic Millimetre-wave Frequency Selective Surfaces', *Anten. and Prop. Soc. Int. Symp. (APSURSI)*, July 2010, pp. 1-4.
9 Kirsch, N., Vacirca, N., Kurzweg, T., Fontecchio, A., and Dandekar, K.: 'Performance of Transparent Conductive Polymer Antennas in a MIMO ad-hoc Network', *Wireless and Mobile Computing, Networking and Comms. (WiMob), 2010 IEEE 6th Int. Conf.*,Oct. 2010, pp. 9-14.
10 Kingsley, N., Anagnostou, M., Tentzeris, M., and Papapolymerou, J.: 'RF MEMS Sequentially Reconfigurable Sierpinski Antenna on a Flexible Organic Substrate With Novel DC-Biasing Technique', *Microelectromechanical Sys., Jrnl of*, 2007,**16**, (5), pp. 1185-1192.
11 NXP Semiconductors: ' BAP50-03 General Purpose PIN Diode - Product Data Sheet', http://www.nxp.com/documents/data_sheet/BAP50-03.pdf. accessed July 2015.
12 Liebig, N.: 'OpenEMS - Open Electromagnetic Field Solver' , http://openEMS.de, accessed June 2015.
13 Mantysalo, M., and Mansikkamaki, P.: 'An Inkjet-Deposited Antenna for 2.4GHz Applications', *AEU- Int Jrnl of Electronics and Comms.*, 2009,**63**,(1), pp. 31-35.